The chemical variability at the surface of Mars: implications for exogenic processes

C. Kolb[1,2], J.A. Martín-Fernández[3], R. Abart[2,4], H. Lammer[1], S. Thió Fernández de Henestrosa[3], and V. Pawlowsky-Glahn[3]

[1]Space Research Institute, Austrian Academy of Sciences, Schmiedlstrasse 6, A-8042 Graz, Austria; *christoph.kolb@oeaw.ac.at*

[2]Institute for Earth Sciences, University of Graz, Universitätsplatz 2, A-8010 Graz, Austria

[3]Department for Computer Science and Applied Mathematics, University of Girona, Campus Montilivi, E-17071 Girona, Catalonia (Spain)

[4]Dept. of Earth Sciences, Free University Berlin, Haus N, Malteserstr. 74 -100, 12249 Berlin, Germany

Abstract

The chemical composition of sediments and rocks, as well as their distribution at the Martian surface, represent a long term archive of processes, which have formed the planetary surface. A survey of chemical compositions by means of Compositional Data Analysis represents a valuable tool to extract direct evidence for weathering processes and allows to quantify weathering and sedimentation rates. *clr*-biplot techniques are applied for visualization of chemical relationships across the surface ("chemical maps"). The variability among individual suites of data is further analyzed by means of *clr*-PCA, in order to extract chemical alteration vectors between fresh rocks and their crusts and for an assessment of different source reservoirs accessible to soil formation. Both techniques are applied to elucidate the influence of remote weathering by combined analysis of several soil forming branches. Vector analysis in the Simplex provides the opportunity to study atmosphere surface interactions, including the role and composition of volcanic gases.

Kew words: Mars, soil, weathering, log-ratio methodology.

1 Introduction

Concerning global tectonics the present day Mars is considered as a single plated planet (Banerdt and others, 1992). Due to the lack of consumptive plate tectonics the regolith, which accumulated at the Martian surface, represents a long-term archive of exogenic processes and contains a record of the evolution of surface conditions on ancient Mars. A number of chemical and physical processes have been invoked in the context of regolith formation including palagonitization (Gooding and Keil, 1978; Morris and others, 1993; Bishop and others, 1998; McSween and Keil 2000; Schiffman and others, 2000; Morris and others, 2001; Bishop and others, 2002a; Schiffman and others, 2002), hydrothermal alteration (Newsom, 1980; Griffith and Shock, 1995; Newsom and others, 1999), and acid fog weathering (Clark and Baird, 1979; Banin and others, 1997; Tosca and others, 2004). Also physical weathering (aeolian activity of abrasion and mixing, e.g. Bridges and others, 1999; Greeley and others, 2002, 1999, 1982; freeze thaw, salt weathering, e.g. Rodriguez-Navarro, 1998) and the accumulation of meteoritic matter (Gibson, 1970; Clark and Baird, 1979; Boslough, 1988a, 1988b; Flynn and McKay, 1990; Flynn, 1996; Yen, 2001) have been addressed.

The primary source of information upon the processes - which were active especially on ancient Mars - can be identified, are data on the chemical and mineralogical compositions of Martian surface materials. Therefore, we are searching for signs of distinctive surface processes in the variability pattern of chemical data, obtained by Mars Pathfinder (NASA) and the Mars Exploration Rover missions (NASA).

In this study we make use of the steadily growing data base on chemical and mineralogical analyses from the Martian surface. We employ *clr* (*centered log ratio*) transformation prior to factor determination in order to take the closed nature of chemical data into account and to prevent bias on the factor loadings obtained (Aitchison, 1986; Aitchison and others, 2000; Aitchison and Greenacre, 2002; Martín-Fernández and others, 2003; Aitchison and others, 2005). Focus is given on visualization of data variability by means of biplot techniques. Based on the variability patterns, rock alteration and soil formation processes such as remote weathering are derived and discussed.

2 Methods

Aitchison (1986) defined a composition to be a collection of *D* non-negative measurements which sum to unity (or 100%) per weight, volume, or abundance. Such constraints are obeyed by the Simplex space geometry, which represents a *D* dimensional analogue of a triangle, in contrast to the *D* dimensional orthogonal Euclidean space geometry. If not all the material originally present in the samples is represented, such collections of data are termed as subcompositions, closed to constant sums (Aitchison, 1986).

The APXS[1] X-ray mode is insufficient to measure oxygen contents and oxide analyses were reported in normalized form (closed to 100%) in order to compensate for variations imposed by measurement geometries of the sensor heads (Brückner and others, 2003; Gellert and others, 2004; Rieder and others, 2004). In contrast, Foley and others (2003) determined oxygen contents on Pathfinder samples via the α-proton mode of APXS and assigned minor influence to various measurement geometries. However, the total amount of iron in soils and rocks was reported in terms of Fe_2O_3 and FeO, respectively, and excess oxygen was assigned to water before analyses were normalized to 100%. In the frame of the Mars Exploration Rover missions Mössbauer spectroscopy was applied to the samples along with APXS, allowing to account for oxygen related to the ferric state, but providing no unequivocal clue to oxygen bound in water and to elements below the limit of detection of APXS. Due to these reasons only subcompositions are available for equivalent comparison of data obtained by the missions under consideration. Because the correlation coefficients between fixed pairs of elements are changed strongly by the closure operation, classical multivariate techniques, such as conventional correspondence analysis or biplot techniques, fail in preservation of the correlations in the covariance structure and, hence, are insufficient for visualization of compositional data sets (Aitchison, 1997). Larsen and others (2000) applied correspondence analysis in Euclidean notation on Viking 1 and Pathfinder soil and rock compositions with the consecution that the closed nature of compositional data has not been sufficiently appreciated.

Aitchison (1986) provide the technique of *clr* transformation, applied to a *D*-compositional vector *C* prior to multivariate treatment, to avoid unfavourable effects associated with closure [Eq. (1)].

$$clr(C) = \left[\log\left(\frac{c_1}{Gn(C)} \right), \ldots, \log\left(\frac{c_D}{Gn(C)} \right) \right] \tag{1}$$

Individual compositional entries c_i are normalized by the geometric mean *Gn(C)* of the vector *C*. Aitchison and others (2000) and Aitchison and others (2005) apply the log-ratio concept to several multivariate techniques of compositional data analysis. Such techniques are denoted by: *clr*-biplot or *clr*-principal component analysis.

2.1 Compositional data and vectors in the Simplex notation

An important consequence of the constrained Simplex space is the dependence of individual compositional entries on each other. This can be directly observed by active change of an individual entry in a data set – e.g. due to metasomatic effects or selective migration of elements between individual solids: the other entries are changing passively due to closure. To account for the relative nature of compositional data, ratios among individual entries are considered rather than absolute values (e.g. Martín-Fernández, 1998). The relative nature of compositional data does not only hold for individual observations, but it is also implicit in the vector, which links different compositions. The ratios between parts of the Simplex vector are a measure of change for the ratios between the same parts of individual observations linked by this vector. The only difference to a common vector in the traditional Euclidian space is that compositional ratios among parts, rather than absolute compositional values, are considered. Application of Simplex vectors to compositions makes sure that the new composition remains in the Simplex space (e.g. Aitchison and others 2000). The "uniform" composition *e* in the *D*-dimensional space Simplex is given by Equation (2). This "uniform" composition *e* corresponds to the barycenter of the Simplex and plays the same role as the origin in the Euclidean space. A compositional vector can be applied to this composition *e* (and, in general, to any

[1] APXS… Alpha Particle X-ray Spectrometer onboard Mars Pathfinder and Mars Exploration Rover mission.

$$e = \left[\frac{1}{D},...,\frac{1}{D}\right] \quad (2)$$

other composition) several times in a multiplicative way – perturbation operation 'o'– until target compositions are reached. The final composition is obtained by normalization – or closure – to 100 % (Aitchison, 1986). If a vector entry is equal to 1/*D* (arithmetic mean), it could seem that the compositional value is invariant from a numerical point of view. But this is not the case. The key to understand variations in the Simplex geometry is the geometric mean of the vector, because it considers the vector as an integrity (Aitchison 1986). More active change of compositions takes place if values of the corresponding vector entries are more different to the geometric mean. Vector entries which are above this level are actively increasing, values which are below are actively decreasing. However, a passive change of compositional values could occur, although the corresponding values of vector entries equal the geometric mean. This is due to the effect of closure on data (Aitchison 1986).

In classical geochemistry, the so called Isocon plot is commonly used to distinguish between active and passive changes of components (e.g. Grant, 1986; Baumgartner and Olsen, 1995). In the following example this graphical concept is reconciled with numerical treatments given in Aitchison (1986). The observation x=[40 25 15 20] is perturbed by the vector p=[21 48 21 10] in order to derive composition *pox*. The geometric mean of the vector is Gn(p)=21.45 and $p_1=p_3=21$. Consequently, x_1 and x_3 should change only passively and in the same proportion. Single application of p on x yield *pox*=[32.88 46.97 12.33 7.83]. The ratio $x_3/x_1=pox_3/pox_1=0.375$, because $p_1/p_3=1$.

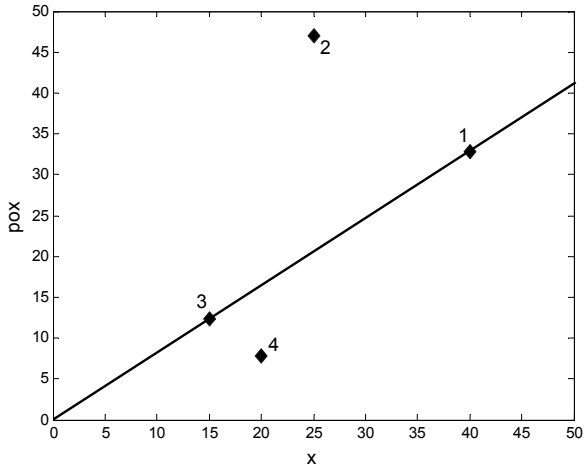

Figure 1: Isocon plot for observation x and the perturbed observation *pox*.

In Figure 1 the Isocon plot of x vs. *pox* is shown. Those points, which are located on a line through the origin, are changed only passively, the others are changed actively, depending on their relative position to the line. Parts 1 and 3 are located on this line, which is consistent with arguments from above.

2.2 *clr*-biplot techniques and *clr*-principal component analysis (PCA)

Biplot techniques provide a means for simultaneous visualization of correlations between multiple variables and observations on a single two-dimensional plot. For the visualization of the correlations between compositional data and variables biplot techniques are used on *clr* transformed data. PCA on *clr* transformed data is used to determine principal component vectors, which best describe the variability of the compositional data.

Chemical compositions of Martian surface materials in terms of element wt% of 13 elements (Na, Mg, Al, Si, P, S, Cl, K, Ca, Ti, Cr, Mn, Fe) were taken from the literature (Mars Pathfinder: Brückner and others, 2003; Foley and others, 2003; MER-A: Gellert and others, 2004; MER-B: Rieder and others, 2004). Viking samples were excluded from our multivariate analysis, because five elements (Na, P, K, Cr, Mn) were not measured. Concentration data on volatile components and on O, Ni, Zn and Br are available only for few missions and samples so that these elements could not be considered in our statistical analysis. In some Pathfinder samples Cr and Mn contents are below the detection limits (approximately

0.1%) of the analytical method used (Brückner and others, 2003). In order to meet the requirements of strictly positive entries for *clr* transformation, missing data for Cr and Mn were replaced by 0.065%, i.e. 65% of the detection limit, after Martín-Fernández and others (2003).

The principal component vectors obtained by *clr*-PCA may be considered as a set of orthogonal compositional vectors, which best describe the variablity of the data set. They are deduced from the eigenvalues and corresponding eigenvectors of the covariance matrix of the *clr* data set. The eigenvalue is a measure of the potential of the corresponding eigenvector to describe data variability. Consequently, the *clr* eigenvectors that correspond to the highest eigenvalues are considered as principal components (Aitchison and Greenacre 2002). Equation (3) shows the relationships between first *clr* eigenvectors of *clr*-PCA and first *clr*-based vector Vec_1 from *clr*-biplot. Vec_1 explains most of variability across the *clr*-biplot (Aitchison and Greenacre 2002).

$$PCA_1 = \frac{Vec_1}{norm(Vec_1)} \tag{3}$$

The *clr* eigenvector PCA_1 represents the unitary vector of the first *clr*-based vector in the *clr*-biplot. The $norm(Vec_1)$ is identical with the first singular value s_1 in the biplot. The first singular value s_1 of the *clr*-biplot is related to the first eigenvalue e_1 of *clr*-PCA by Equation (4), whereby n denotes the number of observations considered.

$$e_1 = \frac{s_1^2}{n-1} \tag{4}$$

The principal *clr* vectors are transformed back into the Simplex per inverse *clr* transformation. A detailed description of deduction of principal vectors in order to describe maximum variability is given in Gower and Hand (1996).

3 Results

3.1 Interrelation among samples and classification

Figure 2 represents a *clr*-biplot. The proportion of total variability explained by the biplot is 74%, which is reasonably high. This figure shows a scheme to discern different classes of samples. The vectors denote the distribution of *clr* transformed variables across the chemical variability of Martian surface materials. The origin of vectors represents the origin in the *clr* transformed Euclidian space. Five classes of sample suites are discernable: Domain of soil, MER-B evaporites, MER-B basalts, MER-A basalts and Mars Pathfinder andesites. The soils are plotting close to the origin. The presumed source rocks are located distal from soils, which is consistent with the observation of chemical uniformity among soils in contrast to rocks (e.g. Brückner and others, 2003; Foley and others, 2003; Rieder and others, 2004; Gellert and others, 2004). The trends allow discrimination between coated and abraded rocks which are located proximal and distal to the vicinity of soils, respectively. The rock “Mazatzal” represents an exception in this respect. The untreated rock and the brushed rock plot in the vicinity of soils and do not fall on the basaltic branch (Fig. 2). However, (twice) abraded rock analyses of “Mazatzal” plot on the trend line. Bishop and others (2002b) developed a model of dust encrustation on rock surfaces, which is based on physical and chemical interaction with airborne dust. Most probably the veneer of “Mazatzal” is cemented dust as a product of such chemical interactions. This is consistent with microscopic information obtained on the rock “Mazatzal” (McSween and others, 2004).

The magmatic rocks are plotting on the side of *clr*(Si) and the evaporites are located in the area spanned by *clr*(S), *clr*(Cl), and *clr*(Mg). The suite of magmatic rocks are subdivided further by their affinity to elements with principal component characteristics. MER-A basalts plot in the vicinity of *clr*(Mg) and *clr*(Cr); andesites are shifted toward majority of *clr*(K) and *clr*(Si); MER-B basalts are of intermediary character. Overall, these observations are consistent with petrological models of Martian rocks (e.g. McSween and others, 2004 and Rieder and others, 2004 regarding MER-A and MER-B basalt, respectively; Minitti and Rutherford, 2000 regarding Mars Pathfinder andesites). The shift between brushed MER-A basalts and abraded MER-A basalts indicates the formation of chemical weathering crusts different from fresh rocks (Fig. 2).

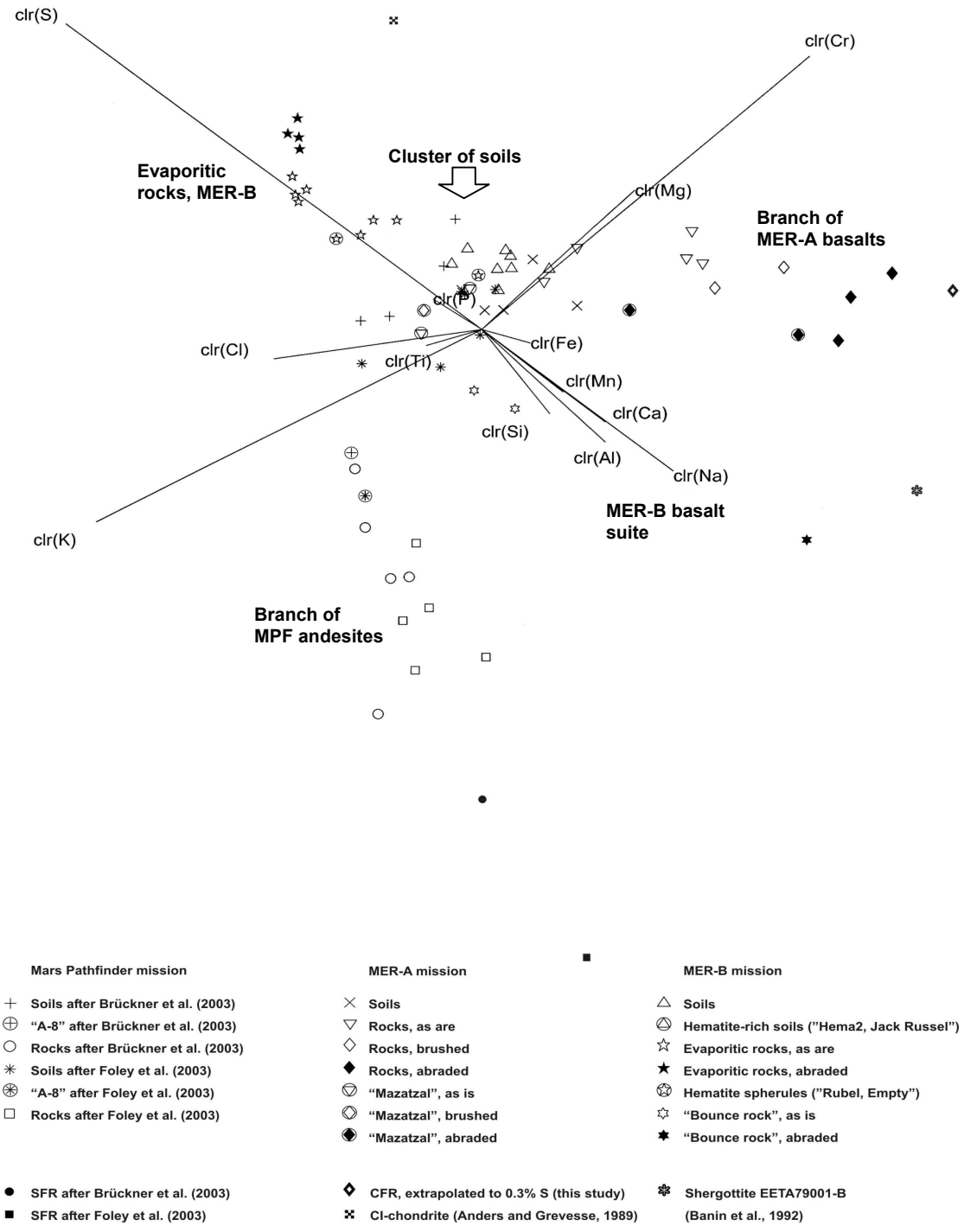

Figure 2: Gross classification of Martian samples, visualized by means of *clr*-biplot techniques on the basis of 13 elements (Na,Mg,Al,Si,P,S,Cl,K,Ca,Ti,Cr,Mn,Fe). The abbreviation SFR and CFR stands for Soil Free Rock and Crust Free Rock, respectively.

3.2 Compositional vector analysis

The deduction of vectors is based on *clr*-PCA. Several vectors are under consideration: alteration vectors between the MER-A basaltic crust and fresh rock, soil formation vectors along the MER-A basaltic branch, along the andesitic branch and among MER-B basalts.

3.2.1 Analysis of alteration vectors in MER-A basalts

The alteration vector calculation is based on *clr*-PCA of fresh basalts (abraded) and their crusts (brushed rocks). The data cloud consists of 5 data sets (rock moiety "Adirondack": "Brush", "RAT"; rock moiety "Humphrey": "Brush", "RAT1", "RAT2"; Gellert and others, 2004). Rock moiety "Mazatzal" ("Brush", "RAT1", "RAT2") was finally excluded because of interferences of crust and pronounced, indurated dust/soil cover on brushed rocks (McSween and others, 2004 and Figure 2). The vector explains 82% of variability and is given in Table 1 in Simplex notation (closed to 100%). The de-alteration vector represents the reciproke, or inverse, alteration vector. Figure 3 shows the alteration and de-alteration vector. The relation of vector entries to the geometric mean is a measure for their degree of change. The element Na remains actively unchanged, the others change to different degree. S and Cl is incorporated in the crust, while Mg and Fe is removed from crust in relation to the fresh rock. This is consistent with the formation pathway of Mg-, Fe-bearing sulfates and ferric oxides upon dissolution of Mg-, Fe-bearing primary silicates). The element K in crusts stems most probably from impurities, derived from remote weathering of andesitic or other K-bearing rocks (see below). The term remote weathering describes the influence of distant weathering on local environments (e.g. Bishop and others, 2002b). The results concerning basalt alteration are consistent with experimental studies on acid fog weathering (Tosca and others, 2004; Banin and others, 1997 and below).

The de-alteration vector was applied to average crust (geometric mean of "Adirondack-Brush" and "Humphrey-Brush") until S reached 0.3 and 0.1% in order to derive Crust Free Rock. The target value of S = 0.3% represents the average value of sulfur in basaltic SNC meteorites (Brückner and others, 2003). The alternative value of S = 0.1% is based on the amount of sulfur in the basaltic SNC meteorite Shergotty (Lodders, 1998). The result is shown in Table 2, whereby the 0.3% extrapolation is comparable to data given in McSween and others (2004).

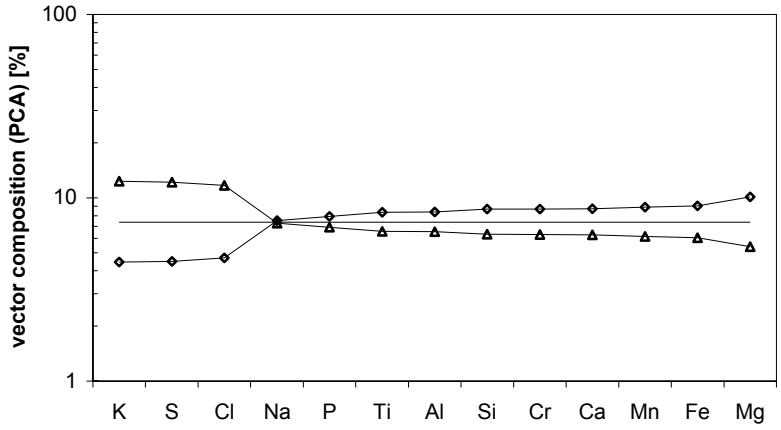

Figure 3: Simplex vectors along alteration trends of MER-A basalts. The vectors are based on inverse *clr*-transformation of *clr*-PCA eigenvectors and are given for both directions. Elements are sorted with increasing values (diamonds) and decreasing values (triangle) to the right. Alteration vector from fresh rock to crust (triangle). The inverse vector (de-alteration) holds for the path from crust to rock (diamond). The geometric mean of vectors is given as horizontal line as reference level.

3.2.2 Soil formation vector along the MER-A basaltic branch

clr-PCA technique was applied to the whole MER-A basalt and soil data complex (Gellert at al., 2004) to derive soil formation vectors which are capable to explain high levels of variability (94%). The vector composition is given in Table 1 in Simplex notation, which shows the sharp increase for S, K, Cl and on the other side the decrease of Cr and Mg. It shows that S, K, and Cl in soils may originate from other sources than the basalts, whereby S and Cl may be associated to volcanic gas and K to weathering of andesites. The main difference to the alteration vector (Table 1) is the different behavior of Cr and Fe. Although Cr does not change intensely along the alteration vector it is strongly changed along the whole basaltic branch, because MER-A basalts may be the main source of Cr in the soil, vice versa is valid for Fe.

Table 1. Simplex vectors along alteration trends of MER-A basalts and along numerous soil formation pathways. The vectors are based on inverse *clr*-transformation of *clr*-PCA eigenvectors and are given for both directions. Gn denotes the geometric mean of vectors as reference level.

	rock alteration (MER-A)		soil formation					
	alteration	de-alteration	MER-A➡ soil	soil➡MER-A	MPF➡ soil	soil➡ MPF	MER-B➡ soil	soil➡ MER-B
Na	7.20	7.50	6.76	8.12	5.08	10.78	6.86	7.98
Mg	5.26	10.31	5.97	9.18	10.19	5.38	6.48	8.45
Al	6.44	8.42	6.20	8.85	6.04	9.07	6.31	8.68
Si	6.21	8.73	6.48	8.45	6.02	9.11	6.18	8.86
P	6.84	7.92	7.73	7.09	8.12	6.75	6.34	8.65
S	12.56	4.31	12.67	4.32	10.78	5.08	13.25	4.13
Cl	12.00	4.52	10.82	5.06	7.80	7.02	13.78	3.98
K	12.68	4.27	12.03	4.56	4.93	11.12	9.10	6.02
Ca	6.16	8.79	6.03	9.10	6.33	8.66	5.98	9.16
Ti	6.46	8.39	7.64	7.17	7.52	7.29	6.37	8.60
Cr	6.19	8.75	5.21	10.50	13.05	4.20	6.70	8.18
Mn	6.04	8.97	6.13	8.94	6.79	8.07	6.29	8.71
Fe	5.94	9.13	6.34	8.64	7.35	7.46	6.38	8.59
Gn	7.33	7.40	7.38	7.42	7.39	7.42	7.36	7.44

Table 2. comparison of Crust Free Rock (this study) with data given in McSween and others (2004). The rock data were extrapolated to S = 0.1 and 0.3% S. Iron was partitioned in Fe^{3+} and Fe^{2+} according to results of Mössbauer spectroscopy on Adirondack and Humphrey (Morris and others, 2004). A and H denotes theoretical rock end-members of Adirondack and Humphrey after McSween and others (2004).

	CFR (0.1% S)	CFR (0.3% S)	A	H
SiO_2	43.8	45.4	45.4	46.1
TiO_2	0.42	0.46	0.46	0.52
Al_2O_3	9.69	10.6	10.9	10.6
Fe_2O_3	3.37	3.26	3.02	2.99
Cr_2O_3	0.58	0.60	0.60	0.59
FeO	15.9	15.4	15.2	15.3
MnO	0.38	0.38	0.41	0.39
MgO	16.0	12.9	12.8	12.2
CaO	7.33	7.52	7.49	7.70
Na_2O	1.92	2.50	2.79	2.59
K_2O	0.01	0.04	0.06	0.06
P_2O_5	0.44	0.53	0.52	0.56
S	0.10	0.30	0.30	0.30
Cl	0.03	0.09	0.09	0.11
TOTAL	100	100	100	100

3.2.3 Soil formation vector along the andesitic branch

Application of *clr*-PCA to the Mars Pathfinder (MPF) andesitic rock and soil branch (Brückner and others, 2003; Foley and others, 2003) provided a vector with 92% explanation of variability. The vector along the andesitic branch probably reflects coating, only. Alteration is not covered by the data set, because abraded andesites were not analyzed. However, as the vector of the basaltic arm mirrors the alteration vector in basalts, some evidence for andesite weathering should be extractable from analysis of the vector along the andesite branch. The composition of the vector in Simplex geometry is given in Table 1. The elements Cr and Mg may be from sources different from andesites but may stem from remote weathering of basaltic materials. The elements K, Na, Si, Al, Ca are released to the soil – most probably by weathering of feldspars and/or feldspathoid glasses in andesites. This is consistent with the formation of KCl, NaCl, Ca- and Al-sulfates and secondary silica or kaolinite (typical weathering products of Na,K feldspar under S,Cl acidic environment). The formation of NaCl, Ca-sulfates and amorphous silica was observed by means of acid fog weathering experiments on rocks with Mars Pathfinder andesite composition (Tosca and others, 2004; Banin and others, 1997).

3.2.4 Soil formation vector along the MER-B basaltic branch

The determination of the vector along the MER-B basalt branch by means of *clr*-PCA is based on three rock datasets (rock sample moieties "Glanz2 (as is), Case (RAT), Red Herring Maggie (as is)", Rieder and others, 2004). The vector covers 99% of variability and is shown in Table 1. The elements Cl, S, K may stem from other sources than MER-B basalts. The dominant release of Si and Ca from MER-B basalts and of Mg and Cr from MER-A basalts is consistent with the finding that MER-B basalts - as analogues to shergottites (Zipfel and others, 2004) - are higher differentiated rocks than MER-A basalts (McSween and others, 2004).

4 Discussion

Figure 4 shows a barycentric projection of K and *Gn*(S,Cl), *Gn*(Mg,Cr) subcompositions and is hence a representation of Simplex geometry. Subcompositions (S,Cl) and (Mg,Cr) are given as geometric means. The MER-A basaltic branch is bent in Figure 4. This indicates some sort of disruption along the vectors and probably reflects different trends associated with physical coating and formation of chemical weathering crusts. Abraded basalts are relatively poor in potassium, which implies that potassium was

most probably provided to the global dust via remote weathering of andesites and has been distributed by the global activity of winds. The trend from andesites to the soil (andesitic branch) does not show the feature of disruption (Fig. 4). This is probably due to the fact that the andesitic branch is not complete due to absence of analyses on abraded andesites in the frame of the Mars Pathfinder mission.

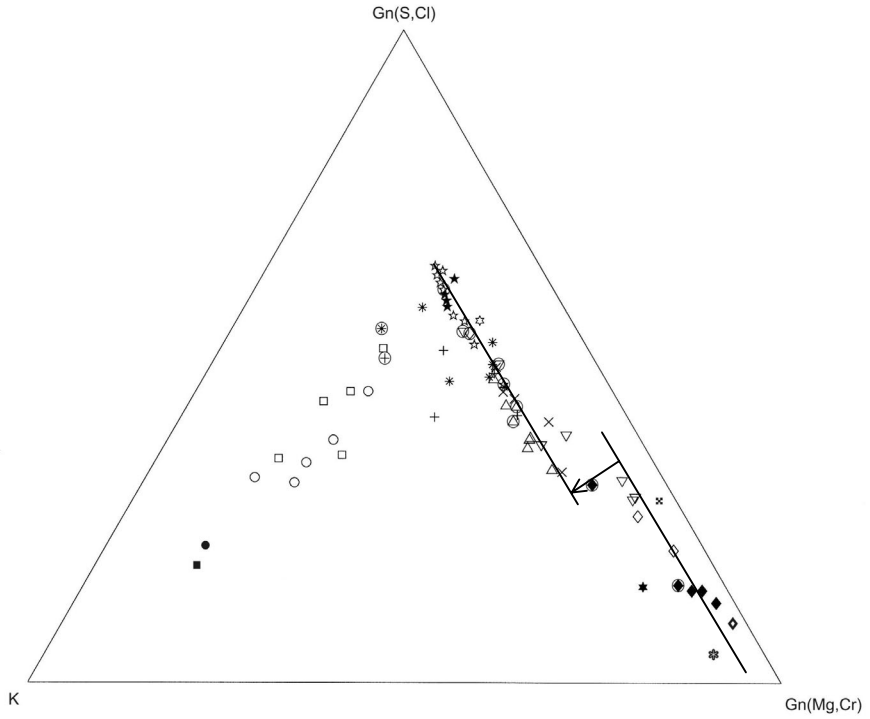

Figure 4: This ternary diagram shows the relationships between Pathfinder mission and MER-A, MER-B missions. Significantly lower K is present in brushed and abraded in relation to coated MER-A basaltic rocks (offset marked by arrow): this may indicate that K bearing phases were deposited in the rinds and did not originate from basalt but from remote weathering of andesites. The array of soils is located at relatively Mg- and Cr-rich compositions which gives evidence that basaltic materials dominate the soils. Legend as Figure 2.

4.1 Alteration vector

Banin and others (1997) and Tosca and others (2004) performed leaching experiments on sediments and synthetic rocks with various acidic solutions in order to study acid fog weathering scenarios. Tosca and others (2004) synthesized rocks and glasses with chemistries according to Mars Pathfinder rock (andesitic) and Mars Pathfinder soil (basaltic) on a S- and Cl-free basis. Many secondary minerals were found by means of Scanning Electron Microscopy (SEM), coupled with Energy Dispersive X-ray spectroscopy (EDS) after evaporation of solutions. Several types of Mg, Fe, Ca and Al bearing sulfates were identified and precipitation of ferric oxides under relatively high pH values (buffered by basalt dissolution) was observed. Throughout the synthetic evaporites and residual crusts secondary, amorphous silica was recognized, which is in general agreement with prediction of sedimentary silica existing on Mars by McLennan (2003). Tosca and others (2004) emphasize that presence of olivine is needed to release large amounts of Mg into solution and that rocks with higher amounts of Si release lower amounts of cations due to higher degree of structural polymerization. Banin and others (1997) performed similar experiments on partly palagonized volcanic tephras and subsequent analysis of secondary mineralogy by means of X-ray Diffraction (XRD). The latter authors reported release of Fe, Al and Mg, but identified only crystalline Al- and Ca-sulfates, because of restrictions of XRD method on crystallinity.

The observations of chemical fractionation between fresh MER-A basalts and their crusts fit very well to the experimental findings given above. Following the hypothetical assumption that fresh rocks can be derived by addition of solutions (originally leached from fresh rocks) to rock crusts, the de-alteration vector given above is a direct measure for the chemical composition of solutions extracted from Martian rocks. The molar ratio of Mg/Si in the vector equals 1.4 (after Table 1). Tosca and others (2004) performed leaching experiments on synthetic basalts with Mars Pathfinder soil chemistry by means of acidic agents (H_2SO_4 + HCl with S/Cl = 4) and derived similar ratios in solutions. Similarity is also given

concerning the dominance of Mg over Ca and Fe in the solution. Tosca and others (2004) ascribe the dominance of Mg in the solutions to dissolution of olivine. Olivine was recovered as rock forming mineral in MER-A basalts (McSween and others, 2004).

4.2 Relationships along andesitic and MER-A basaltic branch and the composition of volcanic gases

Compositional vector analysis represents an useful tool to unravel the relationships among different interacting vectors and serves as an excellent medium to predict un-recovered source reservoirs. The following approach starts with the assumption that Martian soils are composed exclusively from andesites

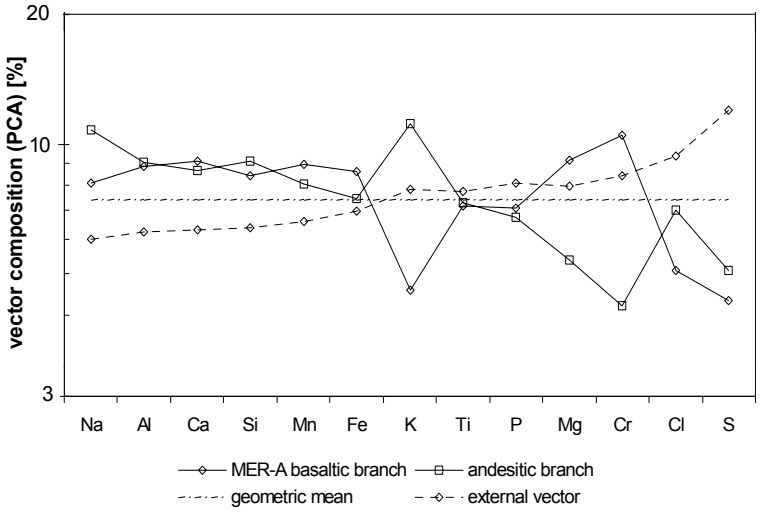

Figure 5: Comparison of vectors along MER-A basaltic and andesitic branch (see text). The data are based on inverse *clr* transformation of first *clr*-PCA vectors. The vector composition is sorted, so that ratios of $\{Gn(a)*Gn(b)\}/\{a[c_i]*b[c_i]\}$ increase to the right. The tendency to compositional symmetry is anticipated, which is consistent with remote weathering effects. The external vector maintains full compositional symmetry between MER-A basaltic and andesitic branch.

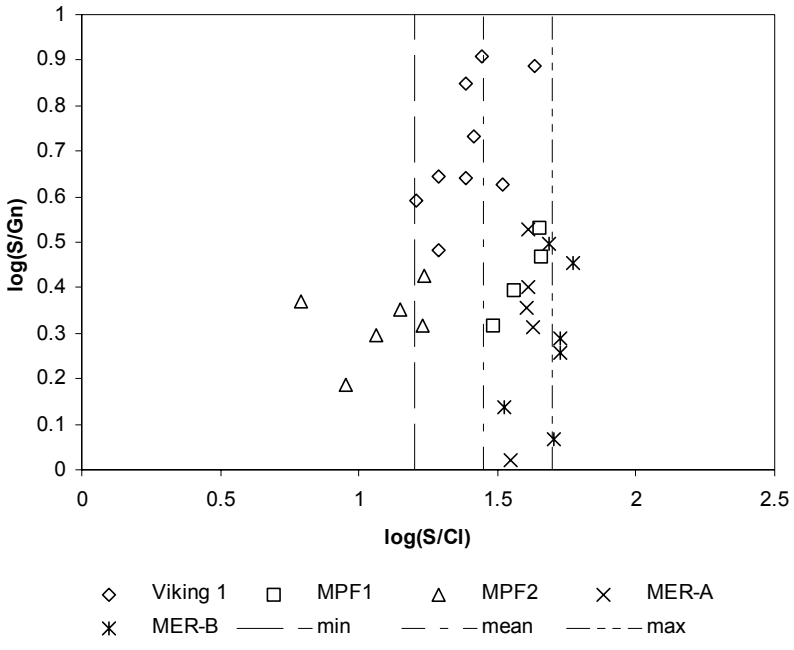

Figure 6: Log-ratio contrast on S and S/Cl ratios in selected soils (MPF1 after Brückner and others, 2003; MPF2 after Foley and others, 2003; without "A-8" hardpan soil; MER-A after Gellert and others, 2004; MER-B after Rieder and others, 2004; Viking 1 after Clark and others, 1982). The calculation of mean, minimum and maximum of *clr*(S/Cl) is based on the assumption of normal distribution (see text).

and MER-A basalts. In such a case the Simplex vectors of andesitic (*a*) and MER-A basaltic branch (*b*) would complement each other in the form of Equation (5).

$$\begin{aligned} a^{-1} &= b, \\ b^{-1} &= a \end{aligned} \tag{5}$$

Subsequently, this case of compositional symmetry will be tested in order to predict hitherto undetermined source reservoirs. In fact, such additional sources are very likely: volcanic gases, other rock types and meteoritic matter. Figure 5 shows a comparison of vectors *a* and *b*. The clearly visible skewness in relation to the common geometric mean (chain dotted line) indicate interaction of external vectors with the andesite-MER-A basalt system. Deduction of the external vector is achieved by deriving the inverse vector of geometric means between vectors *a* and *b* (Fig. 5). Application of such a vector to both branches maintains full compositional symmetry among them. Comparison of the compositional value of S to the geometric mean of the external vector indicates an intense increase of S due to addition of volcanic gas. Potassium is close to the geometric mean and, hence, remains actively unchanged. However, rock reservoirs are still needed, which are rich in Cr, Mg and poor in plagioclase component. Addition from meteoritic sources and basalts may account for these materials. Such rocks contain Cl at modest level, only. Thus, increase in Cl has to be assigned to volcanic gas. The log-ratio contrast on the soil data in Figure 6 gives evidence for mean ratio S/Cl=4.26 with a range based on standard deviation between 3.33 and 5.46.

5 Conclusions

In order to understand the role of acid fog weathering and meteoritic accumulation compositional data analysis was performed on chemical compositions of Martian surface materials. Compositional data analysis by means of *clr*-biplot visualization techniques provides a clear separation of Martian surface samples with context of relationships to elements with principal component characteristics: andesites are related to K, Si; MER-A basalts are related to Mg, Cr; MER-B basalts are of intermediary nature and MER-B evaporites are related to S, Cl, Mg. Overall, these findings are consistent with existing petrological models of Martian rocks. Furthermore, chemical weathering rinds are observed to be significant differently composed in relation to soil and fresh rock, but appear as intermediate stage of soil formation.

Compositional vector analysis provides clues on soil formation pathways and rock alteration trends. The deduction of alteration vectors in MER-A basalts shows the release of Mg and Fe species upon attack of volcanic gases (S, Cl) and acid fluids, which is consistent with models and experiments on acid fog weathering of olivine-bearing basaltic rocks. Similarity is drawn between the molar Mg/Si ratio (1.4) in solutions derived from leaching of synthetic olivine-bearing basalts with Pathfinder soil composition (Tosca and others, 2004) and de-alteration vectors of MER-A basalts in this study, implying past chemical weathering of olivines at the MER-A landing site. The de-alteration vector was applied to average crust in order to derive Crust Free Rock chemistry consistent with existing estimations of MER-A rock end-members (McSween and others, 2004) for the sake of redundancy.

Soil formation vectors originating from andesitic and MER-A basaltic sources are compositional symmetric in their relative appearance, which indicate global interference via remote weathering by adherence of K-chlorides and Mg-sulfates on basalts and andesites, respectively. An external vector gives indications for volcanic gas composition and additional rock reservoirs such as meteoritic matter and basalts. The volcanic gas composition is deduced from log-ratio contrast of S vs. S/Cl in Martian soils (min/mean/max = 3.3/4.3/5.5).

Acknowledgements

This work has received a financial support from the Dirección General de Investigación of the Spanish Ministry for Science and Technology through the project BFM2003-05640/MATE.

References

Aitchison, J. (1986). *The statistical analysis of compositional data*, Chapman and Hall, London, 416 p. Reprinted in 2003 by The Blackburn Press, Caldwell, NJ.

Aitchison, J. (1997). The one-hour course in compositional data analysis or compositional data analysis is simple. In: *Proceedings of IAMG'97*, Pawlowsky-Glahn, V. (ed.), *The Third Annual Conference of the Int. Ass. For Math. Geol.,* Barcelona, Spain, 1, 3-35.

Aitchison, J., Greenacre, M. (2002). Biplots of compositional data. *Applied Statistics*, 51, 375-392.

Aitchison, J., Barceló-Vidal, C., Martín-Fernández, J.A., Pawlowsky-Glahn, V. (2000). Logratio analysis and compositional distance. *Math. Geol.,* 32, 271-275.

Aitchison, J., Kay, J.W., Lauder, I.J. (2005). *Statistical concepts and applications in clinical medicine*, Chapman & Hall/CRC, Boca Raton, 339 p. (ISBN 1-58488-208-5).

Anders, E., Grevesse, N. (1989). Abundances of the elements: Meteoritic and solar. *Geochim. Cosmochim. Acta* 53, 197-214.

Banerdt, W.B., Golombek, M.P., Tanaka, K.L. 1992. Stress and Tectonics on Mars. In: Kieffer, H.H. *et al.* (Eds.), *Mars*, Univ. of Arizona Press, Tucson, 594-625.

Banin, A., Clark, B.C., Wänke, H. (1992). Surface chemistry and mineralogy In: Kieffer, H.H. *et al.* (Eds.), *Mars*, Univ. of Arizona Press, Tucson, 594-625.

Banin, A., Han, F.X., Kan, I., Cicelsky, A. (1997). Acidic volatiles and the Mars Soil. *J. Geophys. Res.* 102, 13,341-13,356.

Baumgartner, L.P., Olsen, S.N. (1995). A least-squares approach to mass transport calculations using the Isocon method, *Econ. Geology*, 90, 1261-1270.

Bishop, J.L., Fröschl, H., Mancinelli, R.L. (1998). Alteration processes in volcanic soils and identification of exobiologically important weathering products on Mars using remote sensing. *J. Geophys. Res.* 103, 31,457-31,476.

Bishop, J.L., Schiffman, P., Southard, R.J. (2002a). Geochemical and mineralogical analyses of palagonitic tuffs and altered rinds of pillow lavas on Iceland and application to Mars. In: Smellie, J.L., Chapman, M.G. (Eds.), *Volcano-Ice Interactions on Earth and Mars, Geol. Soc. Am. Spec. Paper* 202, 371-392.

Bishop, J.L., Murchie, S.L., Pieters, C.M., Zent, A.P. (2002b). A model of dust , soil, and rock coatings on Mars: Physical and chemical processes on the Martian surface. *J. Geophys. Res.* 107, 5097, doi:10.1029/2001JE001581.

Boslough, M.B. (1988a). Evidence for meteoritic enrichment of the Martian regolith. *Lunar Planet. Sci.* XIX, 120-121 (abstr.).

Boslough, M.B. (1988b). Selective weathering of shocked minerals and chondritic enrichment of the Martian fines. *MEVTV Workshop on Nature and Composition of Surface Units on Mars. LPI Tech. Rep.* 88-05, 28-30 (abstr.).

Bridges, N.T., Greeley, R., Haldemann, A.F.C., Herkenhoff, K.E., Kraft, M., Parker, T.J., Ward, A.W. (1999). Ventifacts at the Pathfinder landing site. *J. Geophys. Res.* 104, 8595-8615.

Brückner, J., Dreibus, G., Rieder, R., Wänke, H. (2003). Refined data of Alpha Proton X-ray Spectrometer analyses of soils and rocks at the Mars Pathfinder site: Implications for surface chemistry. *J. Geophys. Res.*, 108 (E12) ROV 35-1, CiteID 8094, DOI 10.1029/2003JE002060.

Clark, B.C., Baird, A.K. (1979). Is the Martian lithosphere sulphur rich? *J. Geophys. Res.* 84, 8395-8403.

Clark, B.C., Baird, A.K., Weldon, R.J., Tsusaki, D.M., Schnabel, L., Candelaria, M.P. (1982). Chemical Composition of Martian Fines. *J. Geophys. Res.* 87, 10,059-10,067.

Flynn, G.J. (1996). The delivery of organic matter from asteroids and comets to the early surface of Mars. *Earth, Moon, and Planets* 72, 469-474.

Flynn, G.J., McKay, D.S. (1990). An Assessment of the Meteoritic Contribution to the Martian Soil. *J. Geophys. Res.* 95, 14,497-14,509.

Foley, C.N., Economou, T., Clayton, R.N. (2003). Final chemical results from the Mars Pathfinder alpha proton X-ray spectrometer. *J. Geophys. Res.*, 108 (E12), ROV 37-1, CiteID 8096, DOI 10.1029/2002JE002019.

Gellert, R., Rieder, R., Anderson, R.C., Brückner, J., Clark, B.C., Dreibus, G., Economou, T., Klingelhöfer, G., Lugmair, G.W., Ming, D.W., Squyres, S.W., d'Uston, C., Wänke, H., Yen, A., Zipfel, J. (2004). Chemistry of Rocks and Soils in Gusev Crater from the Alpha Particle X-ray Spectrometer. *Science,* 305, 829-833.

Gibson, E.K. (1970). A comparison of the Spectral Reflectivity of Mars with Oxidized Meteoritic Material. *Icarus,* 13, 96-99.

Gooding, J.L., Keil, K. (1978). Alteration of glass as a possible source of clay minerals on Mars. *Geophys. Res. Lett.,* 5, 727-730.

Gower, J.C, Hand, D.J. (1996). *Biplots*. Chapman & Hall, London, 277 p., (ISBN 0-412-71630-5).

Grant, J.A. 1986. The isocon diagram--a simple solution to Gresens' equation for metasomatic alteration. *Economic Geology*, 81, 1976-1982.

Greeley, R., Bridges, N.T., Kuzmin, R.O., Laity, J.E. (2002). Terrestrial analogs to wind-related features at the Viking and Pathfinder landing sites on Mars. *J. Geophys. Res.* 107, 5005, doi:10.1029/2000JE001481.

Greeley, R., Kraft, M., Sullivan, R., Wilson, G., Bridges, N., Herkenhoff, K., Kuzmin, R.O., Malin, M., Ward, W. (1999). Aeolian features and processes at the Mars Pathfinder landing site. *J. Geophys. Res.* 104, 8573-8584.

Greeley, R., Leach, R.N., Williams, S.H., White, B.R., Pollack, J.B., Krinsley, D.H., Marshall, J.R. (1982). Rate of Wind Abrasion on Mars. *J. Geophys. Res.* 87, 10,009-10,024.

Griffith, L.L., Shock, E.L. (1995). A Geochemical Model for the Formation of Hydrothermal Carbonates on Mars. *Nature*, 377, 406.

Larsen, K.W., Arvidson, R.E., Jolliff, B.L., Clark, B.C. (2000). Correspondence and least squares analyses of soil and rock compositions for the Viking Lander 1 and Pathfinder landing sites. *J. Geophys. Res.*, 105 (E12), 29,207-29,222.

Lodders, K. (1998). A survey of SNC meteorite whole-rock compositions. *Meteoritics & Planetary Science*, 33, Suppl.., 183-190.

Martín-Fernández, J.A., Barceló-Vidal, C., Pawlowsky-Glahn, V. (2003). Dealing with Zeros and Missing Values in Compositional Data Sets. *Math.. Geol.*, 35(3), 253-278.

Martín-Fernández, J.A., Barceló-Vidal, C. Pawlowsky-Glahn, V. (1998). Critical Approach to Non-Parametric Classification of Compositional Data. In: *Advances in Data Science and Classification*. Proceedings of *the sixth Conference of the International Federation of Classification Societies* Rizzi, A. ,Vichi, M. and Bock, H.H. (eds.),, Università La Sapienza (Roma), Springer-Verlag, Berlin (G), 49-56.

McSween, H.Y., Jr., Keil, K. (2000). Mixing relationships in the Martian regolith and the composition of globally homogeneous dust. *Geochim. Cosmochim. Acta* 64, 2155-2166.

McSween, H.Y., Jr., Arvidson, R.E., Bell, J.F., Blaney, D., Cabrol, N.A., Christensen, P.R., Clark, B.C., Crisp, J.A., Crumpler, L.S., Des Marais, D.J., Farmer, J.D., Gellert, R., Ghosh, A., Gorevan, S., Graff, T., Grant, J., Haskin, L.A., Herkenhoff, K.E., Johnson, J.R., Jolliff, B.L., Klingelhoefer, G., Knudson, A.T., McLennan, S., Milam, K.A., Moersch, J.E., Morris, R.V., Rieder, R., Ruff, S.W., de Souza, P.A., Squyres, S.W., Wänke, H., Wang, A., Wyatt, M.B., Yen, A., Zipfel, J. (2004). Basaltic Rocks Analyzed by the Spirit Rover in Gusev Crater. *Science,* 305, 842-845.

Minitti, M.E., Rutherford, M.J. (2000). Genesis of the Mars Pathfinder "sulfur-free" rock from SNC parental liquids. *Geochim. Cosmochim. Acta*, 64, 2535-2547.

Morris, R.V., Golden, D.C., Bell, J.F., III., Lauer, H.V., Jr., Adams, J.B. (1993). Pigmenting agents in Martian soils - Inferences from spectral, Moessbauer, and magnetic properties of nanophase and other iron oxides in Hawaiian palagonitic soil PN-9. *Geochim. Cosmochim. Acta* 57, 4597-4609.

Morris, R.V., Golden, D.C., Ming, D.W., Shelfer, T.D., Jørgensen, L.C., Bell, J.F., III, Graff, T.G., Mertzman, S.A. (2001). Phyllosilicate-poor palagonitic dust from Mauna Kea Volcano (Hawaii): A mineralogical analogue for magnetic Martian dust? *J. Geophys. Res.* 106, 5057-5083.

Morris, R.V., Klingelhöfer, G., Bernhardt, B., Schröder, C., Rodionov, D.S., de Souza, P.A., Yen, A., Gellert, R., Evlanov, E.N., Foh, J., Kankeleit, E., Gütlich, P., Ming, D.W., Renz, F., Wdowiak, T., Squyres, S.W., Arvidson, R.E. (2004). Mineralogy at Gusev Crater from the Mössbauer Spectrometer on the Spirit Rover. *Science*, 305, 833-837.

Newsom, H.E. (1980). Hydrothermal alteration of impact melt sheets with implications for Mars. *Icarus* 44, 207-216.

Newsom, H.E., Hagerty, J.J., Goff, F. (1999). Mixed hydrothermal fluids and the origin of the Martian soil, *J. Geophys. Res.* 104, 8717-8728.

Rieder, R., Gellert, R., Anderson, R.C., Brückner, J., Clark, B.C., Dreibus, G., Economou, T., Klingelhöfer, G., Lugmair, G.W., Ming, D.W., Squyres, S.W., d'Uston, C., Wänke, H., Yen, A., Zipfel, J. (2004). Chemistry of Rocks and Soils at Meridiani Planum from the Alpha Particle X-ray Spectrometer. *Science,* 306, 1746-1749 [DOI: 10.1126/science.1104358].

Rodriguez-Navarro, C. (1998). Evidence of honeycomb weathering on Mars. *Geophys. Res. Lett.* 25, 3249-3252.

Schiffman, P., Southard, R.J., Eberl, D.D., Bishop, J.L. (2002). Distinguishing palagonitized from pedogenically-altered basaltic Hawaiian tephra: mineralogical and geochemical criteria. In: Smellie, J.L., Chapman, M.G. (Eds.), *Volcano-Ice Interactions on Earth and Mars,* Geol. Soc. Am. Spec. Paper 202, 393-405.

Schiffman, P., Spero, H.J., Southard, R.J., Swanson, D.A. (2000). Controls on palagonitization versus pedogenic weathering of basaltic tephra: Evidence from the consolidation and geochemistry of the Keanakako'i ash member, Kilauea volcano. *Geochem. Geophys. Geosys.* 1, paper no. 2000GC000068.

Tosca, N.J., McLennan, S.M., Lindsley, D.H., Schoonen, M.A.A. (2004). Acid-sulfate weathering of synthetic Martian basalt: The acid fog model revisited. *J. Geophys. Res.*, 109 (E5), CiteID E05003.

Yen, A.S. (2001). Composition and Color of Martian Soil from Oxidation of Meteoritic Material. *32nd Lunar and Planetary Science conference.* Abs. #1766.

Zipfel, J., Anderson, R., Brückner, J., Clark, B.C., Dreibus, G., Economou, T., Gellert, R., Klingelhöfer, G., Lugmair, G.W., Ming, D., Rieder, R., Squyres, S.W., D'Uston, C., Wänke, H., Yen, A., The Athena Science Team (2004). APXS Analyses of Bounce Rock - The First Shergottite on Mars. *Meteoritics & Planetary Science*, 39, Supplement. *Proceedings of the 67th Annual Meeting of the Meteoritical Society, August 2-6, Rio de Janeiro, Brazil*, Abs. #5173.